ORIGINAL ARTICLE

Journal of Cachexia, Sarcopenia and Muscle 2021; **12**: 1741–1756
Published online 25 August 2021 in Wiley Online Library (wileyonlinelibrary.com) **DOI:** 10.1002/jcsm.12770

Pim1 knockout alleviates sarcopenia in aging mice via reducing adipogenic differentiation of PDGFRα+ mesenchymal progenitors

Guo-kai Shang[1†], Lu Han[1,2†], Zhi-hao Wang[1,3], Ming Song[1], Di Wang[1], Yan-min Tan[1], Yi-hui Li[1,4], Yu-lin Li[1], Wei Zhang[1] & Ming Zhong[1*]

[1]*The Key Laboratory of Cardiovascular Remodeling and Function Research, Chinese Ministry of Education, Chinese National Health Commission and Chinese Academy of Medical Sciences, The State and Shandong Province Joint Key Laboratory of Translational Cardiovascular Medicine, Department of Cardiology, Qilu Hospital, Cheeloo College of Medicine, Shandong University, Jinan, Shandong, China;* [2]*Department of General Practice, Qilu Hospital, Cheeloo College of Medicine, Shandong University, Jinan, Shandong, China;* [3]*Department of Geriatric Medicine, Qilu Hospital, Cheeloo College of Medicine, Shandong University; Shandong key Laboratory of Cardiovascular Proteomics, Jinan, Shandong, China;* [4]*Department of Critical Care Medicine, Qilu Hospital, Cheeloo College of Medicine, Shandong University, Jinan, Shandong, China*

Abstract

Background Sarcopenia widely exists in elderly people and triggers numerous age-related events. The essential pathologic change lies in the increased intramuscular adipose tissue after aging with no exception to non-obese objects. Pim1 appears to be associated with adipogenic differentiation in recent studies, inspiring us to explore whether it regulates adipogenesis in aging muscles and affects sarcopenia.

Methods Wild-type and Pim1 knockout C57/BL6J mice were randomized into young and old groups. Histo-pathological and molecular biological methods were applied to assess the intramuscular adipose tissue content, the atrophy and regeneration, and the expressions of Pim1 and adipogenic transcription factors. PDGFRα$^+$ mesenchymal progenitors were separated and their replicative aging model were established. Different time of adipogenic induction and different amounts of Pim1 inhibitor were applied, after which the adipogenic potency were evaluated. The expressions of Pim1 and adipogenic transcription factors were measured through western blotting.

Results The aging mice demonstrated decreased forelimb grip strength ($P = 0.0003$), hanging impulse ($P < 0.0001$), exhaustive running time ($P < 0.0001$), tetanic force ($P = 0.0298$), lean mass ($P = 0.0008$), and percentage of gastrocnemius weight in body weight ($P < 0.0001$), which were improved by Pim1 knockout ($P = 0.0015$, $P = 0.0222$, $P < 0.0001$, $P = 0.0444$, $P = 0.0004$, and $P = 0.0003$, respectively). To elucidate the mechanisms, analyses showed that Pim1 knockout decreased the fat mass ($P = 0.0005$) and reduced the intramuscular adipose tissue content ($P = 0.0008$) by inhibiting the C/EBPδ pathway ($P = 0.0067$) in aging mice, resulting in increased cross-sectional area of all and fast muscle fibres ($P = 0.0017$ and 0.0024 respectively), decreased levels of MuRF 1 and atrogin 1 ($P = 0.0001$ and 0.0329 respectively), and decreased content of Pax7 at the basal state ($P = 0.0055$). In vitro, senescent PDGFRα$^+$ mesenchymal progenitors showed significantly increased the intracellular adipose tissue content (OD510) compared with young cells after 6 days of adipogenic induction ($P < 0.0001$). The Pim1 expression was elevated during adipogenic differentiation, and Pim1 inhibition significantly reduced the OD510 in senescent cells ($P = 0.0040$) by inhibiting the C/EBPδ pathway ($P = 0.0047$).

Conclusions Pim1 knockout exerted protective effects in sarcopenia by inhibiting the adipogenic differentiation of PDGFRα$^+$ mesenchymal progenitors induced by C/EBPδ activation and thus reducing the intramuscular adipose tissue content in aging mice. These results provide a potential target for the treatment of sarcopenia.

Keywords Aging; Pim1; Sarcopenia; Intramuscular adipose tissue; PDGFRα$^+$ mesenchymal progenitors; Adipogenic differentiation

Received: 14 March 2021; Revised: 1 July 2021; Accepted: 10 July 2021

*Correspondence to: Ming Zhong, Department of Cardiology, Qilu Hospital, Cheeloo College of Medicine, Shandong University, Jinan, Shandong 250012, China. Phone: +86 18560086672; Fax: +8653186169356, Email: zhongming2sdu@163.com
†Guo-kai Shang and Lu Han have contributed equally to this work.

Introduction

Sarcopenia is an age-related syndrome characterized by weakened muscle strength and low muscle mass.[1] In the elderly, sarcopenia occurred in 5.5% of men and 13.3% of women,[2] and decreased muscle strength occurred in 74% of people over 85 years old.[3] Sarcopenia leads to several adverse events, including functional limitations, falls, disability, institutionalization, and even death.[4] Thus, it is of great importance to explore its mechanisms.

Increased interstitial adipose tissue in skeletal muscles is a major pathological change of sarcopenia. As ectopic adipose tissue located within muscles,[5] the interstitial adipose tissue changes the muscle microenvironment, induces inflammation and insulin resistance, and negatively affects muscle mass and function.[6,7] As reported, the intramuscular adipose tissue increases by 9–70 g/year,[5] and this increment is an inevitable consequence of aging.[8] Therefore, it is necessary to explore how the adipose tissue increases in aging muscles.

Mesenchymal progenitors are the main source of adipose tissue in skeletal muscles. They are resident multipotent cells of mesenchymal origin in skeletal muscles. They express Sca1, PDGFRα, and CD34 markers and have the potential to differentiate into fibroblasts, adipocytes and osteoblasts.[9,10] Normally, they promote muscle repair by improving the proliferation and differentiation of muscle satellite cells.[11] However, under pathological conditions, they proliferate and differentiate abnormally, resulting in increased fibro-adipose tissue and impaired myogenesis.[12] Multiple studies confirmed that the adipocytes in muscles originate from mesenchymal progenitors,[12] but little has explored their adipogenic capacity after aging. Bone marrow mesenchymal stem cells are of the same origin as muscle mesenchymal progenitors and are reported to have increased adipogenic capacity after aging.[13] Given their homology, senescent muscle mesenchymal progenitors might behave similarly. However, whether their adipogenic capacity increases with aging and the mechanisms remain unclear.

Pim1 may act as a key molecule in regulating the adipogenic differentiation of mesenchymal progenitors. Pim1 is involved in regulating proliferation, apoptosis, differentiation, metabolism, and many other life processes.[14] Through microarray detection, Scimè *et al*. discovered Pim1 was expressed at high levels in aging muscles.[15] Pim1 was highly expressed in adipocyte tumours, but not in non-adipocyte tumours.[16] Besides, Pim1 was associated with fat content in cow muscles.[17] Pim1 inhibitor inhibited adipogenic differentiation of 3T3-L1 pre-adipocytes.[18] All the above-mentioned studies indicated that Pim1 might be a key target regulating the adipogenic differentiation of senescent mesenchymal progenitors.

Herein, we investigated the role of Pim1 in the formation of the interstitial adipose tissue, and its consequent effects on the atrophy and generation of muscle fibres, as well as on the muscle content and strength, and the exercise capacity in wild-type and Pim1 knockout aging mice.

Methods

Animals

Pim1 knockout (Pim1$^{-/-}$) mice (background: C57/BL6J) were established by Model Animal Research Center of Nanjing University using CRISPR/Cas9 techniques. Four-week-old male wild-type (WT) C57/BL6J mice were obtained from Beijing HFK Biotechnology. After the preliminary experiments were conducted and the results were analysed with the PASS software, the sample size was defined as 10 mice per group. Twenty WT and 20 Pim1$^{-/-}$ mice were randomized into young and old groups using the random number table method, and were housed in a temperature-controlled environment under a 12/12 h light–dark cycle with free access to food and water. The young- and old-group mice were raised until they were 3 and 18 months old, respectively, and were used in various assays described later at the end of the experiment.

Dual-energy x-ray absorptiometry body composition analysis

The mice were weighed and anaesthetised, and the limbs were attached to the foam board with the tape. Fat and lean mass were measured by dual-energy x-ray absorptiometry equipment.

Forelimb grip strength test

The mice were trained to grasp the horizontal bar of the horizontally placed dynamometer (Handpi HP-5N, Beijing, China), and were pulled gently backwards until they couldn't fight the pull and release the bar. The force was recorded by the dynamometer. Each mouse was tested trice and the values were averaged.

Hanging grid test

A 45 × 45 cm grid (bar thickness, 2 mm; mesh, 18 mm) and a cushion were respectively placed on and under the frame with a distance of 50 cm between them. The mouse was placed in the grid centre and turned upside down with the mouse head declining first. Hanging time was recorded when the mouse fell off the grid. Hanging impulse was calculated as the product of time and body weight. Each mouse was tested thrice with a >30 min interval between tests and hanging impulse was averaged.

Exhaustive running test

Two days before the test, mice were trained to perform adaptive running on the treadmill twice at a speed of 10 m/min and a slope angle of 0°. On the third day, the exhaustive running test was conducted. The running started at 5 m/min with a slope angle of 0°, and then the speed and slope angle were increased by 5 m/min and 5° every 5 min until they reached 20 m/min and 14°, respectively. The exhaustive running time was recorded when the mouse did not return to the track for >20 s and exhibited obviously diminished response to external stimuli.

Single-muscle function

The mice were anaesthetised and fixed onto a heating plate. Extensor digitorum longus muscle was exposed and separated up to the proximal attachment. The distal tendon was attached to the force transducer by a surgical suture at a low base tension. The muscle was connected to an isolated pulse stimulator (A-M SYSTEMS MODEL 2100, WA, USA) and stimulated at 20 V/cm. The signal was simulated by an A/D converter and recorded by LabChart 5.0 software (ADInstruments, Australia). Five millisecond squared wave stimulation was administered and the base tension was gradually increased until the maximal wave occurred. With the tension maintained, the muscle was stimulated trice with 5 ms pulses at 0.2 Hz, and the maximal isometric twitch forces were recorded and averaged. Then the muscle was stimulated trice with 5 ms pulses at 100 Hz for 300 ms with a 60 s interval between stimulations, and the maximal isometric tetanic forces were recorded and averaged. Subsequently, the muscle was isolated and transected, and the maximal cross-sectional area was determined using a stereoscope (Nikon SMZ25, Japan) and the Image Pro Plus.

Tissue processing

After weighing and anaesthetising, the blood was collected, and the serum was separated. Bilateral gastrocnemius muscles were collected and weighed. One muscle was stored at −80°C after liquid nitrogen treatment. The other was fixed with 4% paraformaldehyde, dehydrated by gradient ethanol series, and embedded with paraffin to make 5 μm sections; or dehydrated by gradient sucrose series, and embedded with optimal cutting temperature compound to make 10 μm sections.

Serological tests

Serum was analysed for free fatty acid (FFA), triglyceride (TG), total cholestero (TC), HDL-C, and LDL-C using the Bayer 1650 blood chemistry analyser (Bayer AG, Leverkusen, Germany) and for adiponectin and leptin using ELISA kits (Proteintech KE10044 and KE10048, USA).

Haematoxylin–eosin staining

After being dewaxed and hydrated, the slides were soaked in haematoxylin for 3 min, washed in running water for 3 min, subjected to 5 s differentiation with 1% hydrochloric acid ethanol, washed in running water for 5 min, soaked in eosin for 2 min, washed in running water for 30 s, dehydrated with ethanol, cleared in dewaxing solution, and finally mounted. The images were acquired using an Olympus DP72 digital imaging system (Olympus Corporation, Tokyo, Japan).

Immunohistochemical staining

The slides were dewaxed and hydrated, and the antigens were retrieved using citric acid buffer at 95–99°C for 20 min (for myosin, fast MyHC, laminin, and adiponectin) or using proteinase K at 37°C for 30 min (for slow MyHC). After treating with 3% hydrogen peroxide and 5% bovine serum albumin, the sections were incubated overnight at 4°C with primary antibodies (from Abcam, UK, or Proteintech, USA): Anti-myosin (ab37484), Anti-Fast Myosin Skeletal Heavy Chain (ab51263), Anti-Slow Myosin Skeletal Heavy Chain (ab11083), Anti-laminin (ab11575), Anti-adiponectin (ab181281), and Anti-perilipin 1 (ab3526). Subsequently, the sections were first incubated with enhancing solution, and then with secondary antibodies. The slides were washed with phosphate buffered solution (PBS) between each of the above-mentioned steps. After adding 3, 3′-diaminobenzidine solution (Wuhan Servivebio Technology G1212, China), the reactions were observed

DOI: 10.1002/jcsm.12770

under a microscope and stopped in distilled water when target area turned yellow. Lastly, the nuclei were stained by haematoxylin, and the slides were dehydrated, cleared, and mounted. The images were acquired using an Olympus DP72 digital imaging system (Olympus Corporation, Tokyo, Japan) and analysed using Image Pro Plus. The size of muscle fibres was represented by cross-sectional area (CSA, i.e. area divided by cell number); the relative content of fast and slow muscle fibres was represented by the number of slow-MyHC-positive fibres divided by the number of fast-MyHC-positive fibres; the content of central nucleated fibres was represented by the number of central nucleated fibres divided by the number of total muscle fibres; the contents of adiponectin were represented by their integrated optical density values.

Oil red O staining

Stock solution was made by dissolving oil red O powder in isopropanol (1 g in 200 ml). Working solution was prepared by mixing stock solution with distilled water (3:2). For tissue sections, after drying and soaking orderly in distilled water and 60% isopropanol, the sections were soaked in working solution for 15 min and the nuclei were stained by haematoxylin. The images were acquired using an Olympus DP72 digital imaging system (Olympus Corporation, Tokyo, Japan) and analysed by Image Pro Plus. Intramuscular adipose tissue content was represented as the ratio of oil red O-positive area to muscle fibre area. For cell experiments, the cells were washed with PBS, fixed by 4% paraformaldehyde, stained by working solution for 15 min, and washed with PBS. The images were captured using a microscope (Nikon, Ti-S, Japan). Then, isopropanol was added to each well to extract the oil red O in cells for 10 min and then transferred to 96-well plates to measure the Optical density at 510 nm (OD510).

Western blotting

Proteins were extracted from gastrocnemius muscles and cells, separated on 10% SDS-polyacrylamide gels, and transferred onto PVDF membranes (Millipore IPVH304F0 and ISEQ00010, USA), which were soaked in 5% skim milk (room temperature, 1 h), washed, and then exposed overnight to primary antibodies (from Cell Signaling Technology, USA; Abcam, UK; or ProteinTech, USA): Anti-Pim1 (D8D7Y), Anti-GAPDH (66004-1-Ig), Anti-GLB1/Beta-galactosidase (ab128993), Anti-p53 (ab26), Anti-p16-INK4A (10883-1-AP), Anti-Fbx32 (ab168372), Anti-TRIM63 (55456-1-AP), Anti-PAX7 (ab199010), Anti-Myogenin (ab1835), Anti-MyoD1 (ab16148), Anti-Myf5 (ab125301), Anti-Adiponectin (ab181281), Anti-PPAR gamma (ab45036), Anti-CEBP Beta (ab32358), Anti-CEBP Delta (ab65081), Anti-FABP4 (ab92501), Anti-SQSTM1p62 (ab109012), and Anti-LC3B (ab192890). Subsequently, the membranes were washed and incubated with horseradish peroxidase-labelled anti-rabbit or anti-mouse (ZSGB-BIO ZB-2305 or ZB-2301, Beijing, China) secondary antibodies at room temperature for 90 min. After being washed, the enhanced chemiluminescence reagent (Millipore WBKLS0500, USA) was added, and the images were acquired and quantified using Image J.

Separation, identification, culture, and adipogenic induction of PDGFRα^+ mesenchymal progenitors

Fresh lower limb muscles of 1-month-old mice were separated. After removing the nerves, vessels, tendons, and adipose tissue, the muscles were minced and digested in 0.2% collagenase Type II solution at 37°C for 90 min. After filtering through 100-μm cell strainers, the cells were centrifuged, resuspended, and cultured in collagen I-coated dishes at 37°C in 5% CO_2 for 10 days using high glucose Dulbecco's modified Eagle's medium supplemented with 20% fetal bovine serum, 2-mM L-glutamine, 1% penicillin–streptomycin, and 2.5 ng/ml basic fibroblast growth factor. Then the cells were scraped off the dishes and blown into single cells. After counting and centrifugation, they were incubated firstly with CD31 and CD45 micro-beads (Miltenyi Biotec 130-097-418 and 130-052-301, Germany) to collect the $CD31^-CD45^-$ cells, and then with FcR Blocking Reagent and PDGFRα micro-beads (Miltenyi Biotec 130-101-547, Germany) to get $CD31^-CD45^-PDGFR\alpha+$ cells. The cells were cultured in a humidified 37°C incubator at 5% CO_2.

Cell purity was identified by immune-fluorescent staining of PDGFRα. Briefly, after being fixed, the cells were incubated with 5% BSA, anti-PDGFRα antibodies, anti-goat fluorescence secondary antibodies, and DAPI in sequence. Images were acquired using the microscope (Nikon, Ni-E, Japan).

The cells were passed once every week, and the medium were changed twice weekly. Cells at Passage 6 and 22 were used as young and senescent cells, respectively. For adipogenic differentiation, cells were cultured with adipogenic medium (MesenCult™ Adipogenic Diff Kit, Stemcell Technologies 05507, Canada) supplemented with 2 mM L-glutamine.

Senescence-associated β-galactosidase activity assay

The cells were washed with PBS, fixed with the fixing solution, and stained by the staining solution (Beyotime C0602, Shanghai, China). Images were acquired using the microscope (Nikon, Ti-S, Japan).

Proliferation assay

Cell proliferation was evaluated using the Cell-Light EdU Apollo567 In Vitro Kit (RiboBio C10310-1, Guangzhou, China). Briefly, the cells were incubated with growth medium containing EdU for 2 h. Then they were fixed with 4% paraformaldehyde, treated with 0.5% TritonX-100, and incubated with Apollo® solution and Hoechst solution. Images were acquired using the microscope (Nikon, Ti-S, Japan).

Statistical analysis

Data are represented as means ± SEM. SPSS 19.0 and GraphPad Prism 6.0 were used for statistical analysis and image presentation. Comparisons among four or more groups were performed using two-way ANOVA and Tukey's tests, whereas comparisons between two groups were performed using unpaired *t* tests. $P < 0.05$ was considered significant.

Results

Pim1 knockout alleviated sarcopenia in aging mice

To determine the influence of Pim1 on sarcopenia, we raised the WT and Pim1 $^{-/-}$ mice until they were 3 or 18 months of age. Western blotting showed that the relative contents of the age-related markers β-galactosidase (GLB1), p53, and p16 in muscles were significantly increased both in WT old mice than in WT young mice ($P = 0.0476$, $P < 0.0001$, and $P < 0.0001$, respectively), and in Pim1$^{-/-}$ old mice than in Pim1$^{-/-}$ young mice ($P = 0.0005$, $P < 0.0001$, and $P > 0.05$, respectively) (*Figure* 1A–D). Pim1 expression was drastically increased in WT old compared with WT young mice ($P = 0.0002$), and decreased in Pim1$^{-/-}$ old compared with WT old group ($P < 0.0001$) (*Figure* 1E,F). The body weight and serological parameters were shown in the figures (*Figure* 1G–N).

Next, we investigated the effects on sarcopenia. WT old mice showed obviously decreased forelimb grip strength, hanging impulse, exhaustive running time, and tetanic force of extensor digitorum longus ($P = 0.0003$, $P < 0.0001$, $P < 0.0001$, and $P = 0.0298$, respectively), which were significantly improved in Pim1$^{-/-}$ old mice ($P = 0.0015$, $P = 0.0222$, $P < 0.0001$,and $P = 0.0444$, respectively) (Figure 2A–E). Dual-energy x-ray analysis revealed that the lean mass was significantly decreased in WT old compared to WT young mice ($P = 0.0008$) and significantly increased in Pim1$^{-/-}$ old compared with WT old mice ($P = 0.0004$) (Figure 2F). Similarly, the percentage of gastrocnemius weight in body weight was lower in WT old compared with WT young group ($P < 0.0001$), and was higher in Pim1$^{-/-}$ old compared with WT old group ($P = 0.0003$) (Figure 2G). The above-mentioned results suggested that Pim1 knockout significantly alleviated sarcopenia in aging mice, but the mechanisms need to be elucidated.

Pim1 knockout alleviated intramuscular adipose tissue infiltration in aging mice

Given that intramuscular adipose tissue increases with age and affects muscle function, we examined whether Pim1 knockout alleviated sarcopenia through reducing intramuscular adipose tissue. Dual-energy x-ray analysis revealed that WT old mice had significantly increased fat mass compared to WT young mice ($P = 0.0007$), whereas Pim1$^{-/-}$ old mice had obviously decreased fat mass compared to WT old mice ($P = 0.0005$) (*Figure* 3A). Similarly, oil red O staining showed that the intramuscular adipose tissue content was significantly increased in WT old compared with WT young mice ($P = 0.0072$), and was significantly decreased in Pim1$^{-/-}$ old compared with WT old mice ($P = 0.0008$) (*Figure* 3B,C). Immunofluorescence staining of perilipin 1 showed that WT old mice had significantly increased content of intramuscular lipid droplets compared with WT young mice ($P < 0.0001$), whereas Pim1$^{-/-}$ old mice had obviously decreased content compared with WT old mice ($P < 0.0001$) (*Figure* 3B,D). Western blotting and immunohistochemical staining of adiponectin indicating adipose tissue content showed similar results ($P < 0.05$ for all) (*Figure* 3B,E–G).

The above-mentioned results indicated that Pim1 knockout reduced the accumulation of intramuscular adipose tissue in aging mice, which might be a key reason for the improvements in the function and mass of aging muscles.

Decreased intramuscular adipose tissue caused by Pim1 knockout alleviated skeletal muscle fibre atrophy and decreased the mobilization of satellite cells at the basal state in aging mice

To figure out why decreased intramuscular adipose tissue caused by Pim1 knockout alleviated sarcopenia in aging mice, we examined its effect on muscle fibre atrophy. Haematoxylin–eosin staining showed marked variations in size and arrangement of muscle fibres in WT old mice, but a comparatively more uniform arrangement in Pim1$^{-/-}$ old mice (*Figure* 4A). The total CSA and the CSA of fast muscle fibres were significantly reduced in WT old compared with WT young mice ($P = 0.0137$ and 0.0194, respectively) and were significantly increased in Pim1$^{-/-}$ old compared with WT old mice ($P = 0.0017$ and 0.0024, respectively). No obvious changes were discovered in the CSA of slow muscle fibres ($P > 0.05$). The ratio of slow to fast muscle fibres was significantly higher in WT old compared to WT young mice

DOI: 10.1002/jcsm.12770

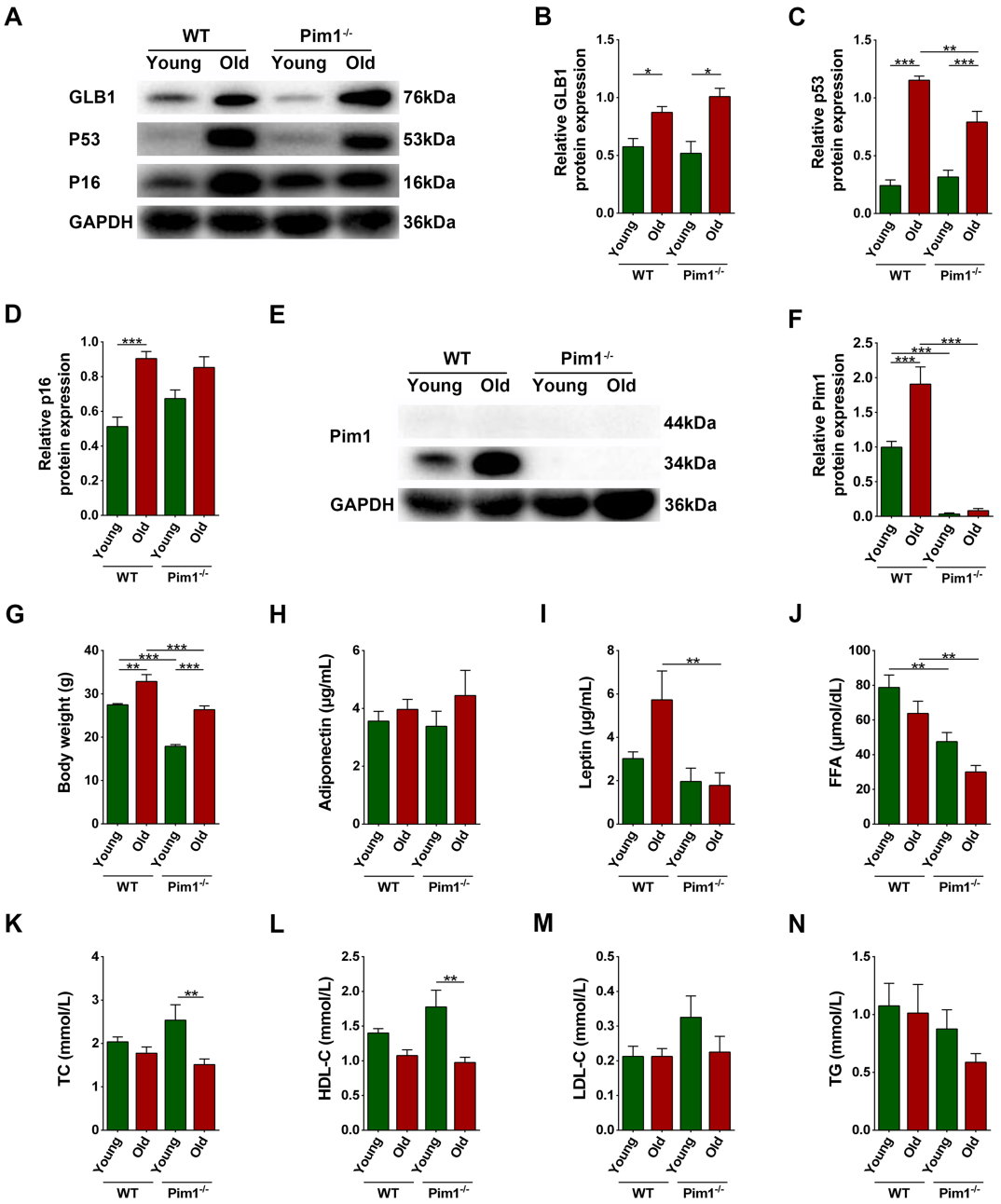

Figure 1 Establishment of natural aging animal model and general examinations. *(A)* Expression of GLB1, p53, and p16 detected through western blotting; GAPDH: internal reference. *(B–D)* Relative protein-expression levels of GLB1, p53, and p16. (e) Expression of Pim1 detected through western blotting; GAPDH: internal reference. (F) Relative protein-expression level of Pim1. (G) Body weight (g). *(H–N)* Contents of adiponectin (μg/mL), leptin (μg/mL), FFA (μmol/dL), TC (mmol/L), HDL-C (mmol/L), LDL-C (mmol/L), and TG (mmol/L) in the murine serum. N = 8–10; *$P < 0.05$, **$P < 0.01$, ***$P < 0.001$ (*Supporting information*, *Data* S1).

(P = 0.0173), and non-significantly lower in Pim1$^{-/-}$ old compared with WT old mice (P = 0.1558) (*Figure* 4A–E). WT old mice had increased levels of MuRF 1 and atrogin 1 compared with WT young mice ($P < 0.0001$ and P = 0.0003, respectively), whereas Pim1$^{-/-}$ old mice had decreased levels compared with WT old mice (P = 0.0001 and 0.0329, respectively) (Figure 4F–H). These results indicated that Pim1 knockout alleviated muscle fibre atrophy in aging mice.

In addition to muscle fibre atrophy, we explored the muscle regeneration at the basal state. WT old mice had increased percentage of central nucleated cells and higher levels of Pax7 and MyoG compared with WT young mice (P = 0.0156,

DOI: 10.1002/jcsm.12770

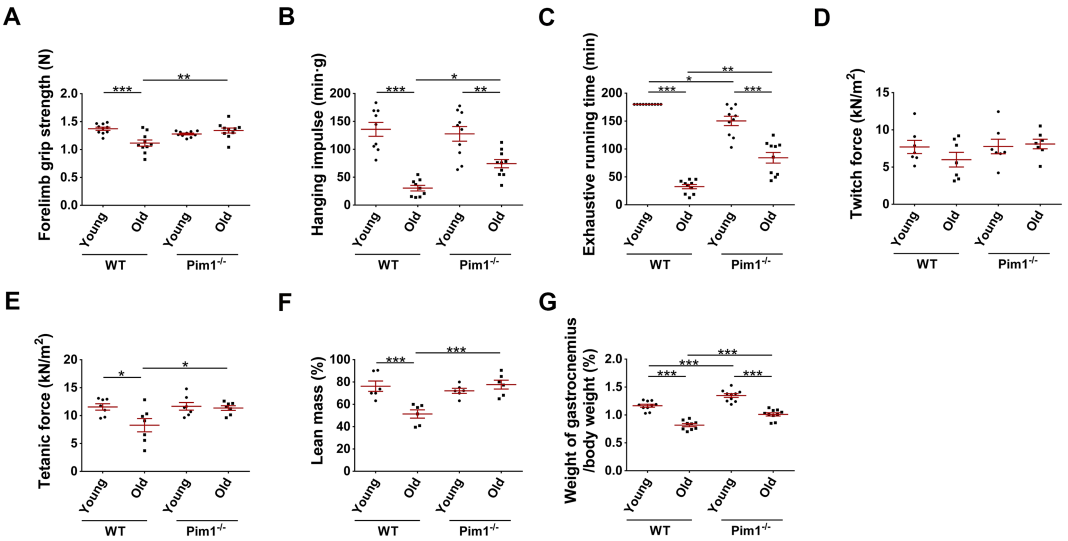

Figure 2 Pim1 knockout alleviated sarcopenia in aging mice. *(A)* Forelimb grip strength (N). *(B)* Hanging impulse (min g). *(C)* Exhaustive running time (min). *(D)* Twitch force (kN/m^2). *(E)* Tetanic force (kN/m^2). *(F)* Lean mass measured through dual-energy x-ray analysis (%). *(G)* Percentage of gastrocnemius weight in body weight (%). N = 6–10; *$P < 0.05$, **$P < 0.01$, ***$P < 0.001$.

$P < 0.0001$, and $P < 0.0001$, respectively), indicating mobilization of muscle satellite cells and activation of muscle regeneration after aging. Pim1 knockout significantly decreased the level of Pax7 (P = 0.0055), indicating decreased mobilization of muscle satellite cells (*Figure* 4A,I–N). Because satellite cell mobilization in the adult muscles usually occurs when there are pathological stimuli that injure the muscles, these results indicated that Pim1 knockout reduced at least some of these pathological stimuli in aging muscles in the basal state. Science-impaired autophagy is shown to be responsible for the behaviour of aged satellite cells, we detected the autophagy of muscles by western blotting. The relative protein levels of p62 and LC3 in skeletal muscles were significantly increased in the WY old group compared with the WT young group ($P < 0.0001$ for both), and were significantly decreased in the Pim1$^{-/-}$ old group compared with the Pim1$^{-/-}$ young group (P = 0.0006 and 0.0003, respectively), indicating that the autophagy flow was inhibited after aging and was improved by Pim1 knockout (*Figure* 4O–Q).

The above-mentioned results suggested that decreased intramuscular adipose tissue caused by Pim1 knockout improved the exercise capacity and muscle function by alleviating muscle fibre atrophy and reducing pathologic stimuli, but the mechanism by which Pim1 knockout reduced intramuscular adipose tissue remained unclear.

Senescent PDGFRα$^+$ mesenchymal progenitors had increased adipogenic potency

Considering that the PDGFRα$^+$ mesenchymal progenitors are the major source of adipocytes in skeletal muscles, we explored whether aging increases intramuscular adipose tissue by influencing the adipogenic potency of these cells. We separated CD31$^-$CD45$^-$PDGFRα$^+$ mesenchymal progenitors using magnetic beads (*Figure* 5A), examined the purity (*Figure* 5B), cultured the cells for 22 passages, and confirmed their aging ($P < 0.05$ for all) (Figure 5C–G). Next, we examined the protein level of Pim1 in young and senescent cells and discovered that senescent cells expressed more Pim1 protein ($P < 0.0001$) (*Figure* 5H,I).

Next, we cultured cells with adipogenic medium for 0, 3, 6 or 9 days. Oil red O staining demonstrated that both young and senescent cells exhibited more intracellular lipids over time. Young cells presented obvious adipogenesis on the 6th day, and reached a peak on the 9th day; whereas senescent cells presented obvious adipogenesis on the 3rd day, and reached a peak on the 6th day (*Figure* 6A). We extracted the oil red O in cells using isopropanol and found that the OD510 was increased over time both in young and senescent groups. In young group, the OD510 reached a peak on the 9th day; while in the senescent group, it reached a peak on the 6th day. On Days 3 and 6, the OD510 was significantly higher in the senescent compared with those of the young group (P = 0.0192 and $P < 0.0001$, respectively) (*Figure* 6B). These results suggested that although young cells eventually held more lipids, senescent cells were more sensitive to adipogenic stimulation.

Next, we examined the changes of adiponectin and adipogenic transcription factors. Following the adipogenic induction, the relative contents of adiponectin, PPARγ, C/EBPβ, C/EBPδ, and FABP4 in young cells were increased in a time-dependent manner and reached peaks on Day 9. In senescent cells, the relative contents were firstly increased with adipogenic differentiation, then reached peaks on Day 6 (except for PPARγ), and finally decreased as the adipogenic

DOI: 10.1002/jcsm.12770

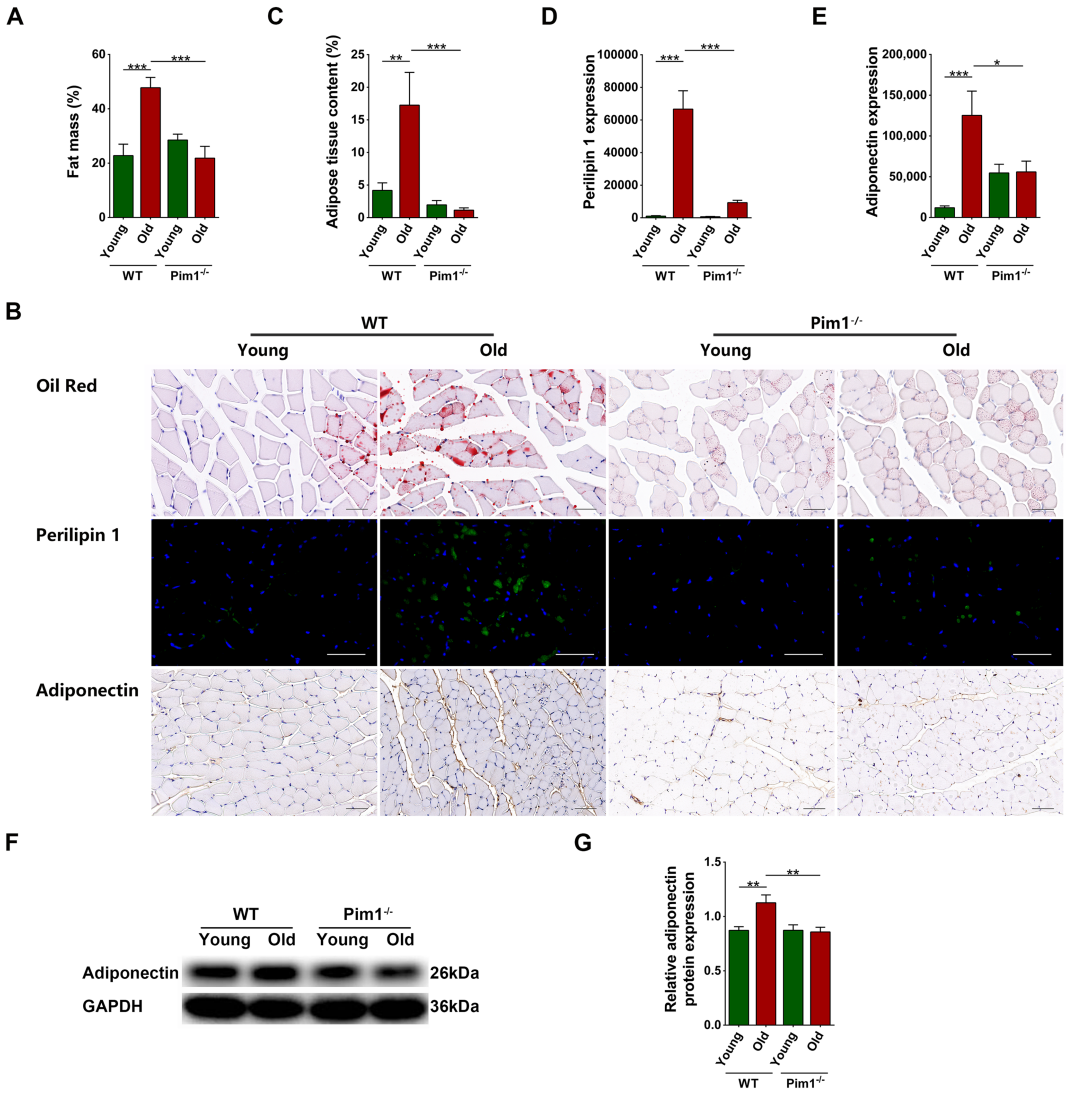

Figure 3 Pim1 knockout alleviated intramuscular adipose tissue infiltration in aging mice. *(A)* Fat mass measured through dual energy x-ray analysis (%). *(B)* Oil red staining, immunofluorescent staining of perilipin 1, and immunohistochemical staining of adiponectin (scale = 50 μm). *(C)* Adipose tissue content (%). *(D)* Immunofluorescent analysis of perilipin 1 expression. *(E)* Immunohistochemical analysis of adiponectin expression. *(F)* Detection of adiponectin expression through western blotting; GAPDH: internal reference. *(G)* Relative protein-expression level of adiponectin. $N = 6–8$; $^{*}P < 0.05$, $^{**}P < 0.01$, $^{***}P < 0.001$.

differentiation ended. On Day 6, the contents of C/EBPβ and C/EBPδ were significantly higher in senescent cells than in young cells ($P < 0.0001$ and $P = 0.0005$, respectively) (*Figure* 6C–H). Considering the above-mentioned results, we chose 6 days as the effective adipogenic induction time.

We then examined the variation of Pim1 content by western blotting. The relative content of Pim1 was increased in young cells over time. Senescent cells expressed high level of Pim1 protein on Day 0. After adipogenic induction, the Pim1 content was firstly decreased possibly because the cells stopped growing, then increased with adipogenic differentiation, and finally decreased as the adipogenic differentiation ended. On Day 6, the Pim1 protein content was significantly higher in senescent cells than in young cells ($P = 0.0264$) (*Figure* 6I–J).

Pim1 inhibitor SGI1776 significantly inhibited the adipogenic differentiation of senescent PDGFRα⁺ mesenchymal progenitors

Given that the changes in Pim1 content were consistent with the adipogenic differentiation process, we ought to verify whether Pim1 intervention affects the adipogenic differentiation. We added different concentrations (2.5 μM/5 μM/10 μM) of Pim1 inhibitor SGI1776 to the adipogenic medium and found that it reduced the formation of intracellular lipids and reduced the OD510 in a concentration-dependent manner. SGI1776 at a concentration of 5 μM was enough to inhibit the adipogenesis of senescent cells ($P = 0.0040$) (*Figure* 7A,B). Ten-μM SGI1776 inhibited adipogenesis more

DOI: 10.1002/jcsm.12770

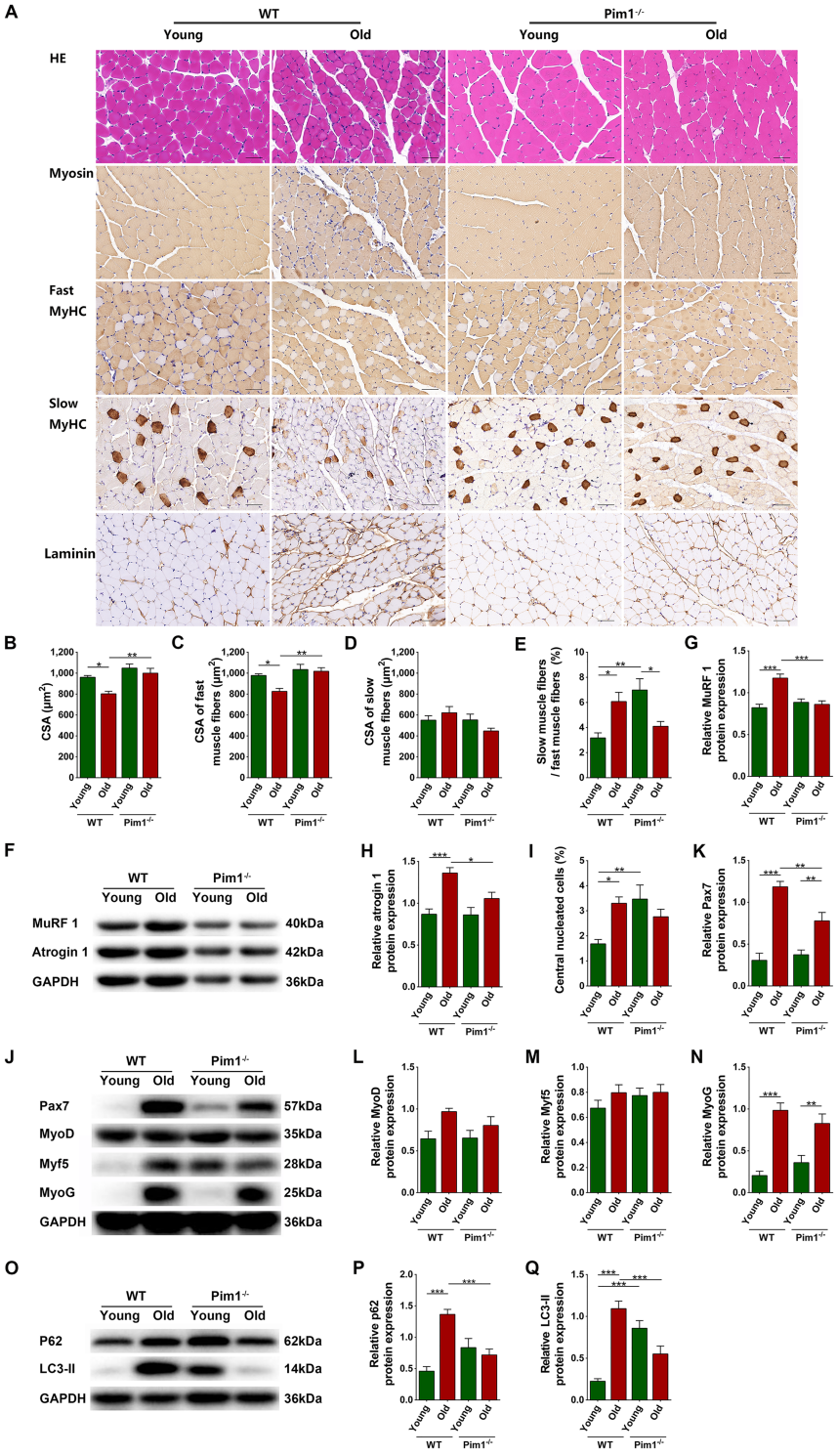

Figure 4 Decreased intramuscular adipose tissue caused by Pim1 knockout alleviated skeletal muscle fibre atrophy and decreased the mobilization of satellite cells at the basal state in aging mice. *(A)* Haematoxylin–eosin (HE) staining and immunohistochemical staining of myosin, fast MyHC, slow MyHC, and laminin (scale = 50 μm). *(B)* Cross-sectional area (CSA) of muscle fibres (μm^2). *(C)* CSA of fast muscle fibres (μm^2). *(D)* CSA of slow muscle fibres (μm^2). *(E)* Ratio of the number of slow muscle fibres to the number of fast muscle fibres (%). *(F)* Detection of MuRF 1 and atrogin 1 expression through western blotting; GAPDH: internal reference. *(G,H)* Relative protein-expression levels of MuRF 1 and atrogin 1. *(I)* Percentage of central nucleated muscle fibres in total muscle fibres (%). *(J)* Detection of Pax7, MyoD, Myf5, and MyoG expression through western blotting; GAPDH: internal reference. *(K–N)* Relative protein-expression levels of Pax7, MyoD, Myf5, and MyoG. *(O)* Detection of P62 and LC3-II expression through western blotting; GAPDH: internal reference. *(P,Q)* Relative protein-expression levels of P62 and LC3-II. $N = 8$; $^*P < 0.05$, $^{**}P < 0.01$, $^{***}P < 0.001$.

DOI: 10.1002/jcsm.12770

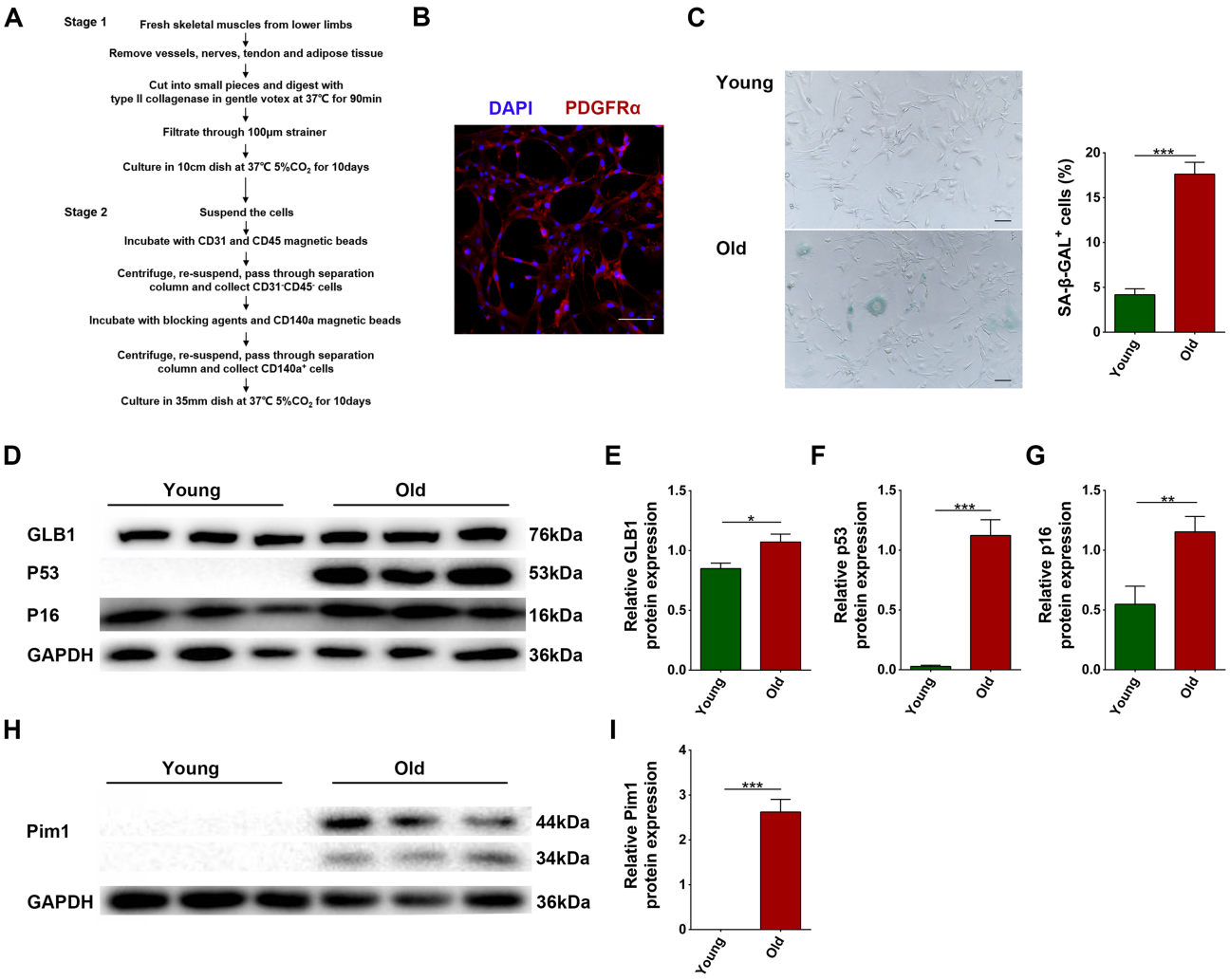

Figure 5 Separation of PDGFRα$^+$ mesenchymal progenitors and establishment of aging model. *(A)* Separation of PDGFRα$^+$ mesenchymal progenitors by magnetic beads. *(B)* Immunofluorescent staining of PDGFRα (scale = 100 μm). *(C)* Senescence associated β-galactosidase staining and content of SA-β-GAL$^+$ cells (%) (scale = 100 μm). *(D)* Detection of GLB1, p53, and p16 expression through western blotting; GAPDH: internal reference. *(E–G)* Relative protein-expression levels of GLB1, p53, and p16. *(H)* Detection of Pim1 expression through western blotting; GAPDH: internal reference. *(I)* Relative protein-expression level of Pim1. $N = 3$; $^*P < 0.05$, $^{**}P < 0.01$, $^{***}P < 0.001$.

obviously, but it was fatal to young cells (data not show). Therefore, 5-μM SGI1776 was used in subsequent experiments. Treatment of 5-μM SGI1776 significantly decreased the content of adiponectin in young cells ($P = 0.0159$) and the amount of secreted adiponectin in young and senescent cells ($P < 0.0001$ for both) (*Figure* 7C–E).

We also evaluated the effects of Pim1 inhibition on the senescence and proliferation of these cells. Pim1 inhibition non-significantly decreased the percentage of SA-β-GAL$^+$ cells ($P = 0.0512$) and significantly decreased the relative protein contents of GLB1, p53, and p16 ($P = 0.0168$, $P < 0.0001$, and $P = 0.0476$) in senescent cells (Figure 7F–K). Edu staining showed that the proliferation of senescent cells was significantly decreased compared to that of young cells ($P = 0.0217$) and Pim1 inhibition significantly inhibited the proliferation of young cells ($P < 0.0001$) (*Figure* 7L,M). These results demonstrated that Pim1 inhibition not only influenced the adipogenic differentiation, but also impacted the senescence and proliferation of PDGFRα$^+$ mesenchymal progenitors.

Pim1 inhibition or knockout reduced the adipogenic differentiation of senescent PDGFRα$^+$ mesenchymal progenitors by inhibiting the C/EBPδ pathway

We examined the effects of Pim1 inhibition on the expression of adipogenic transcription factors in PDGFRα$^+$ mesenchymal progenitors. Senescent cells had decreased levels of PPARγ

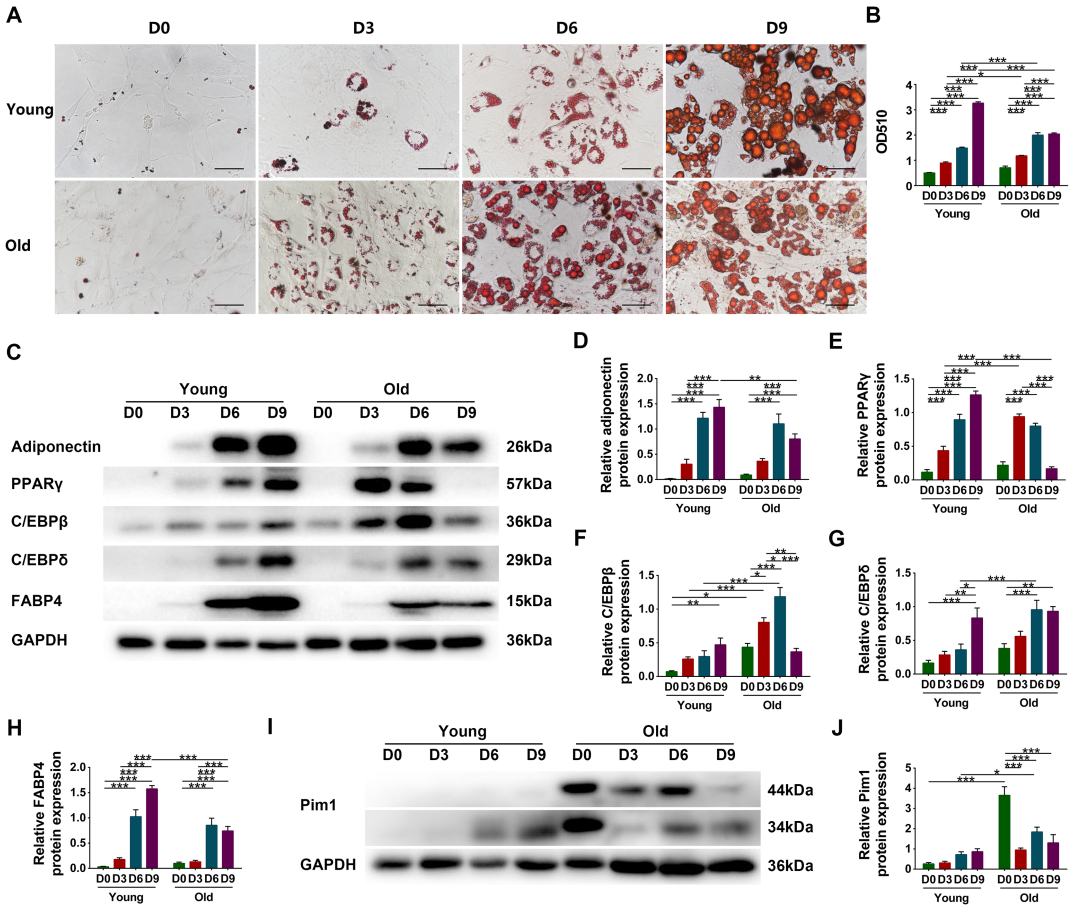

Figure 6 Senescent PDGFRα$^+$ mesenchymal progenitors had increased adipogenic potency. *(A)* Oil red staining of young and senescent PDGFRα$^+$ mesenchymal progenitors after 0 day, 3 days, 6 days, or 9 days adipogenic induction (scale = 50 μm). *(B)* Analysis of OD510. *(C)* Detection of adiponectin, PPARγ, C/EBPβ, C/EBPδ, and FABP4 expression through western blotting; GAPDH: internal reference. *(D–H)* Relative protein-expression levels of adiponectin, PPARγ, C/EBPβ, C/EBPδ, and FABP4. *(I)* Detection of Pim1 expression through western blotting; GAPDH: internal reference. *(J)* Relative protein-expression level of Pim1. N = 3–4; *$P < 0.05$, **$P < 0.01$, ***$P < 0.001$.

and FABP4 and increased levels of C/EBPβ and C/EBPδ compared to young cells ($P < 0.0001$, $P < 0.0001$, $P < 0.0001$, and $P = 0.0027$, respectively); Pim1 inhibition drastically decreased the expressions of PPARγ and FABP4 in young cells and the expressions of C/EBPβ and C/EBPδ in senescent cells ($P < 0.0001$, $P < 0.0001$, $P < 0.0001$, and $P = 0.0047$, respectively), suggesting that Pim1 inhibitor inhibits the adipogenic differentiation of young and senescent cells by interfering with different transcription factors (*Figure* 8A–E). Next, we invested the effects of Pim1 knockout on the expression of the above-mentioned factors in skeletal muscles. WT old mice exhibited increased content of C/EBPδ compared to WT young mice ($P = 0.0054$), whereas Pim1$^{-/-}$ old mice exhibited decreased content compared to WT old mice ($P = 0.0067$) (*Figure* 8F–J). The above-mentioned cellular and animal results demonstrated that C/EBPδ was the key molecule mediating the effect of Pim1 to regulate the adipogenic differentiation of old mesenchymal progenitors.

Discussion

This study showed that Pim1 promoted the adipogenic differentiation of senescent PDGFRα$^+$ mesenchymal progenitors, leading to increased intramuscular adipose tissue, which promoted muscle fibre atrophy, accelerated the consumption of muscle satellite cells, and thus resulted in declined muscle mass, muscle strength, and exercise capacity. Pim1 knockout protected against sarcopenia by inhibiting the adipogenic differentiation in aging muscles.

Decrease of muscle strength, loss of muscle mass, and decline of exercise capacity are the main manifestations of sarcopenia. Accordingly, our study showed that old mice had obvious sarcopenia and increased Pim1 protein expression in the skeletal muscles. Pim1 is the downstream effector of many cytokines and transcription factors. It can be induced by cytokines including IL-6 and transcription factors, such as STAT1α, STAT3, and STAT5,[14,19–20] and is increased in the

DOI: 10.1002/jcsm.12770

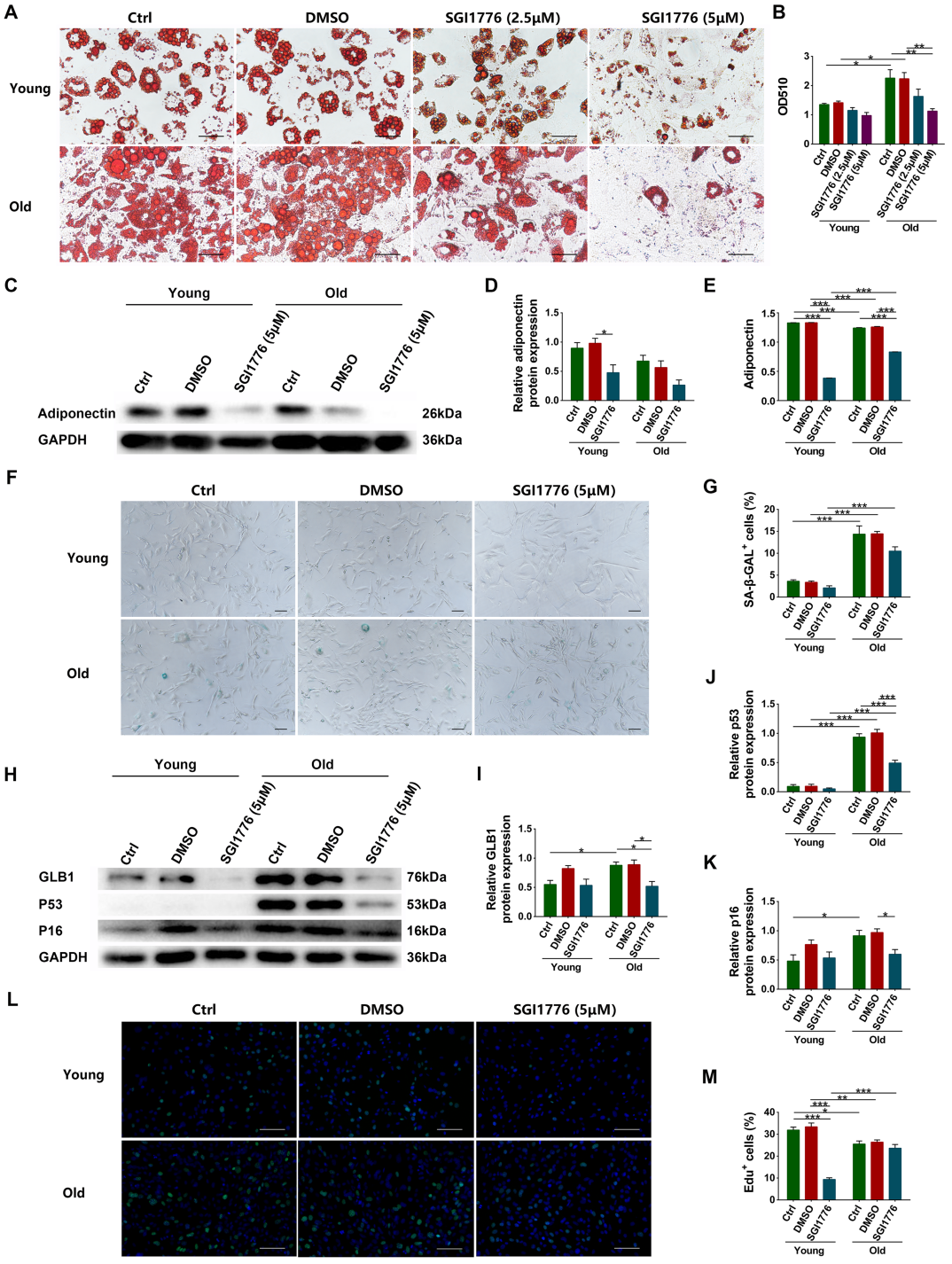

Figure 7 Pim1 inhibitor SGI1776 significantly inhibited the adipogenic differentiation of senescent PDGFRα$^+$ mesenchymal progenitors. *(A)* Oil red staining of young and senescent PDGFRα$^+$ mesenchymal progenitors after 6 days adipogenic induction with different concentrations of SGI1776 (scale = 50 μm). *(B)* Analysis of OD510. *(C)* Detection of adiponectin expression through western blotting; GAPDH: internal reference. *(D)* Relative protein-expression level of adiponectin. *(E)* Adiponectin content in supernatant. *(F)* Senescence associated β-galactosidase staining (scale = 100 μm). *(G)* Content of SA-β-GAL$^+$ cells (%). *(H)* Detection of GLB1, p53, and p16 expression through western blotting; GAPDH: internal reference. *(I–K)* Relative protein-expression levels of GLB1, p53, and p16. *(L)* Edu staining of young and senescent PDGFRα$^+$ mesenchymal progenitors (scale = 100 μm). *(M)* Content of Edu$^+$ cells (%). N = 3–4; *$P < 0.05$, **$P < 0.01$, ***$P < 0.001$.

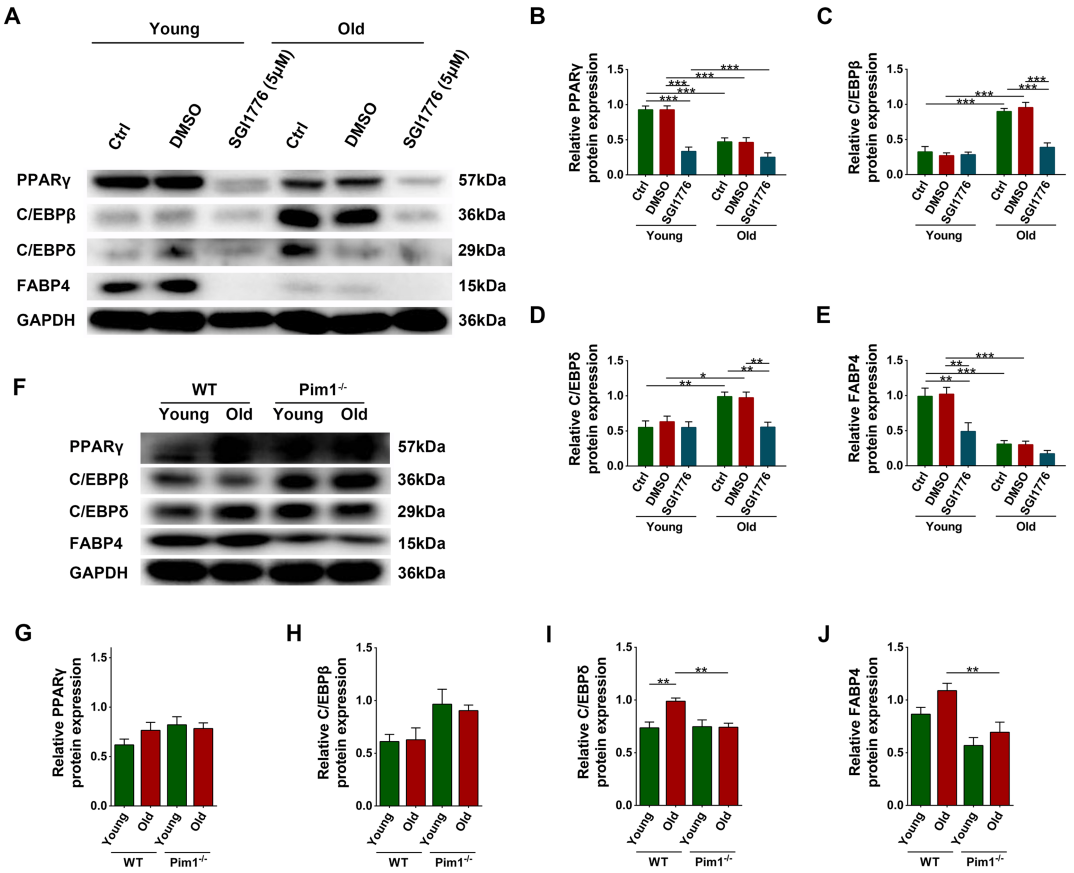

Figure 8 Pim1 inhibition or knockout reduced the adipogenic differentiation of senescent PDGFRα$^+$ mesenchymal progenitors by inhibiting the C/EBPδ pathway. *(A)* Detection of PPARγ, C/EBPβ, C/EBPδ, and FABP4 expression in PDGFRα$^+$ mesenchymal progenitors through western blotting; GAPDH: internal reference. *(B–E)* Relative protein-expression levels of PPARγ, C/EBPβ, C/EBPδ, and FABP4. *(F)* Detection of PPARγ, C/EBPβ, C/EBPδ, and FABP4 expression in murine gastrocnemius muscles through western blotting; GAPDH: internal reference. *(G–J)* Relative protein-expression levels of PPARγ, C/EBPβ, C/EBPδ, and FABP4. $N = 4–8$; $^*P < 0.05$, $^{**}P < 0.01$, $^{***}P < 0.001$.

hypoxia state.[21] The chronic inflammatory state and chronic hypoxia after aging might be the cause for the up-regulation of Pim1 expression. Pim1 is widely involved in the regulation of cell proliferation, apoptosis, differentiation, metabolism, and many other life processes.[14] Thus, a Pim1 knockout aging mouse model was established to evaluate its effects. Pim1 knockout significantly increased the muscle function and content and the exercise capacity of aging mice, indicating a protective role of Pim1 against sarcopenia. It's worth noting that Pim1 knockout almost completely restored the parameters reflecting explosive exercise capacity to normal in aging mice, including the tetanic force of the extensor digitorum longus muscles and the forelimb grip strength, with the parameters reflecting exercise endurance like the inverted hanging impulse and the exhaustive running time not yet fully recovered. This might be related to the fact that Pim1 knockout significantly inhibited the atrophy of the fast muscle fibres, making the CSA almost restored to normal, but had no significant effect on the slow muscle fibres.

Increased intramuscular adipose tissue is a major pathological change for sarcopenia. In our study, the intramuscular adipose tissue content was increased after aging, as previously reported,[22] and was significantly decreased after Pim1 knockout. Considering the passive effects of intramuscular adipose tissue on sarcopenia,[6,23] Pim1 knockout-mediated decrease of intramuscular adipose tissue might be an important reason for the alleviation of sarcopenia. First, increased intramuscular adipose tissue acted as a key promoter for muscle atrophy. As reported, co-culture with 3T3-L1 adipocytes up-regulated the expression of MuRF 1 and Atrogin 1, markers of muscle atrophy, in C2C12 cells[24]; and high-fat diet induced the expression of MuRF 1 and Atrogin 1 in murine muscles.[25] In our study, aging significantly increased, whereas Pim1 knockout significantly reduced the expression levels of Atrogin 1 and MuRF 1 in skeletal muscles; similarly, aging significantly decreased, whereas Pim1 knockout significantly increased the size of fast muscle fibres, demonstrating that Pim1 knockout-induced decrease of intramuscular adipose tissue exerted its anti-sarcopenia effect by inhibiting muscle

fibre atrophy. In addition, increased intramuscular adipose tissue also affected the mobilization of satellite cells at the basal state. Our study showed that aging mice had elevated levels of satellite cell activation marker Pax7 and late myogenesis marker MyoG and increased content of central nucleated cells, which was similar to the results of a previous study on human quadriceps.[26] These results indicated that muscle satellite cells and muscle regeneration pathways are activated in the basal state after aging. Muscle satellite cells normally stay in the resting phase in adulthood and are induced to activate, proliferate, and differentiate in response to injury or pathological stimulations.[27] Their continuous mobilization at the basal state indicates persistent pathological factors in aging muscles. Pim1 knockout significantly decreased Pax7 and non-significantly decreased MyoG and central nucleated cells, suggesting that Pim1 knockout-induced decrease of intramuscular adipose tissue might alleviate sarcopenia by inhibiting some persistent pathological factors. It's worth noting that in the study of Munoz-Canoves *et al*., the function and number of muscle satellite cells in 24-month-old and 28-month-old mice were decreased, which was different from the status of the satellite cells in 18-month-old mice in our study. It was hypothesized that the over-mobilization of muscle satellite cells at the basal state in the early aging stage might be a reason for their excessive depletion and inability to differentiate in the terminal stage. In conclusion, the increase of intermuscular adipose tissue may be an important factor to accelerate the pathological process of sarcopenia. Thus, it is interesting to explore the mechanisms by which Pim1 regulates the intramuscular adipose tissue content.

PDGFRα^+ mesenchymal progenitors are an important source of intramuscular adipocytes.[28–30] As reported, bone marrow-derived and adipose-derived mesenchymal stem cells had enhanced adipogenic differentiation after aging.[31,32] Similarly, our study revealed that muscle-derived senescent mesenchymal progenitors were more sensitive to adipogenic stimulation and formed adipocytes more rapidly, indicating that they had increased adipogenic capacity after aging, which might be the key reason for the increase of intramuscular adipose tissue in aging mice. Further, our study showed that Pim1 expression was increased in senescent mesenchymal progenitors as well as in the process of adipogenic differentiation and Pim1 inhibition significantly inhibited the adipogenic differentiation. Thus, Pim1 played a key role in promoting the adipogenic differentiation of senescent mesenchymal progenitors and thereby increased the intramuscular adipose tissue content in aging mice. However, the mechanisms involved here remain to be further elucidated.

C/EBPβ and C/EBPδ are early regulators of adipogenic differentiation and regulate the expression of PPARγ, which further regulates the expression of FABP4 in late adipogenic stage, forming a cascade to promote adipogenic differentiation.[33] Our study showed that the expression of the above-mentioned adipogenic regulatory factors changed differently during the adipogenic differentiation of PDGFRα^+ mesenchymal progenitors. The levels of PPARγ and FABP4 were significantly increased in young cells, while the levels of C/EBPβ and C/EBPδ were significantly increased in senescent cells. Pim1 inhibition decreased the expression of PPARγ and FABP4 in young cells and the expression of C/EBPβ and C/EBPδ in senescent cells. These results suggested that the inhibitory effect of Pim1 inhibition on the adipogenic differentiation of young and senescent cells depend on different transcription factors, i.e. PPARγ and FABP4 for young cells, and C/EBPβ and C/EBPδ for senescent cells. Further examination in mice showed that C/EBPδ was highly expressed in aging muscles, whereas Pim1 knockout significantly decreased the expression of C/EBPδ. Considering the more complex environmental factors in animals, C/EBPδ might be the key factor that ultimately affects the adipogenic differentiation of PDGFRα^+ mesenchymal progenitor cells in aging mice and was located downstream of Pim1.

Interestingly, although Pim1 intervention in old mice showed a protective effect against sarcopenia, yet the exhaustive running time of Pim1$^{-/-}$ young mice was shorter than that of WT young mice. This might owe to the promoting effect of Pim1 on growth and development. As was shown in our study, 3-month-old Pim1$^{-/-}$ mice were smaller and lighter than WT mice of the same age, suggesting that there might be slight growth retardation. Besides, inhibition of Pim1 was reported to inhibit the differentiation and fusion of C2C12 cells, suggesting that Pim1 might play a role in skeletal muscle development.[34] Yet no obvious myopathy was discovered in 12-week-old Pim1$^{-/-}$ mice.[34] In our study, Pim1$^{-/-}$ young mice had significantly increased central nucleated cells and slightly elevated expression of myogenic transcription factors, further indicating that Pim1 knockout slowed the growth and development to some extent in the young mice, but it did not lead to sarcopenia. After aging, Pim1 knockout increased the cross-sectional area and improved the muscle function, playing a protective role against sarcopenia.

In conclusion, our results suggested that Pim1 promoted the adipogenic differentiation of senescent PDGFRα^+ mesenchymal progenitors by activating the C/EBPδ pathway, resulting in increased intramuscular adipose tissue, which promoted the atrophy of the muscle fibres, accelerated the consumption of the muscle satellite cells, and thus led to the decline of the muscle mass, the muscle strength, and the exercise capacity. Pim1 knockout played a protective role in sarcopenia by inhibiting the adipogenic differentiation in aging muscles. Our study was the first to report the role of Pim1 in the adipogenic differentiation of senescent mesenchymal progenitors and the subsequent effects on sarcopenia in aging mice. Our findings suggested that Pim1 might be a potential intervention target for the prevention and treatment of age-related sarcopenia. Yet the *in-vivo* effects of Pim1 inhibitor would be assessed in the future.

Funding

This work was supported by the research grants from the National Natural Science Foundation of China (81702194, 81801953, and 81700334) and Key Research and Development Programme of Shandong Province (2019GSF108041).

Online supplementary material

Additional supporting information may be found online in the Supporting Information section at the end of the article.

Data S1. Supporting Information

Conflict of interest

The authors declare that they have no conflict of interest.

Ethics statement

The authors of this manuscript certify that they complied with the ethical guidelines for authorship and publishing in the *Journal of Cachexia, Sarcopenia and Muscle*.[35] All animal studies have been approved by the appropriate ethics committee and have therefore been performed in accordance with the ethical standards laid down in the 1964 Declaration of Helsinki and its later amendments. The manuscript does not contain clinical studies or patient data.

References

1. Cruz-Jentoft AJ, Sayer AA. Sarcopenia. *Lancet* 2019;**393**:2636–2646.
2. Shaw SC, Dennison EM, Cooper C. Epidemiology of sarcopenia: determinants throughout the lifecourse. *Calcified Tissue International* 2017;**101**:229–247.
3. Dodds RM, Granic A, Davies K, Kirkwood TB, Jagger C, Sayer AA. Prevalence and incidence of sarcopenia in the very old: findings from the Newcastle 85+ Study. *Journal of Cachexia, Sarcopenia and Muscle* 2017;**8**:229–237.
4. Aversa Z, Zhang X, Fielding RA, Lanza I, LeBrasseur NK. The clinical impact and biological mechanisms of skeletal muscle aging. *Bone* 2019;**127**:26–36.
5. Addison O, Marcus RL, Lastayo PC, Ryan AS. Intermuscular fat: a review of the consequences and causes. *International Journal of Endocrinology* 2014;**2014**:309570.
6. Sachs S, Zarini S, Kahn DE, Harrison KA, Perreault L, Phang T, et al. Intermuscular adipose tissue directly modulates skeletal muscle insulin sensitivity in humans. *American Journal of Physiology. Endocrinology and Metabolism* 2019;**316**:E866–E879.
7. Bruseghini P, Capelli C, Calabria E, Rossi AP, Tam E. Effects of high-intensity interval training and isoinertial training on leg extensors muscle function, structure, and intermuscular adipose tissue in older adults. *Frontiers in Physiology* 2019;**10**:1260.
8. Wang J, Cui C, Chim YN, Yao H, Shi L, Xu J, et al. Vibration and beta-hydroxy-beta-methylbutyrate treatment suppresses intramuscular fat infiltration and adipogenic differentiation in sarcopenic mice. *Journal of Cachexia, Sarcopenia and Muscle* 2020;**11**:564–577.
9. Eisner C, Cummings M, Johnston G, Tung LW, Groppa E, Chang C, et al. Murine tissue-resident PDGFRα+ fibro-adipogenic progenitors spontaneously acquire osteogenic phenotype in an altered inflammatory environment. *Journal of Bone and Mineral Research* 2020;**35**:1525–1534.
10. Stumm J, Vallecillo-Garcia P, Vom Hofe-Schneider S, Ollitrault D, Schrewe H, Economides AN, et al. Odd skipped-related 1 (Osr1) identifies muscle-interstitial fibro-adipogenic progenitors (FAPs) activated by acute injury. *Stem Cell Research* 2018;**32**:8–16.
11. Wosczyna MN, Konishi CT, Perez Carbajal EE, Wang TT, Walsh RA, Gan Q, et al. Mesenchymal stromal cells are required for regeneration and homeostatic maintenance of skeletal muscle. *Cell Reports* 2019;**27**:2029–2035.
12. Collao N, Farup J, De Lisio M. Role of zmetabolic stress and exercise in regulating fibro/adipogenic progenitors. *Frontiers in Cell and Development Biology* 2020;**8**:9.
13. Khorraminejad-Shirazi M, Dorvash M, Estedlal A, Hoveidaei AH, Mazloomrezaei M, Mosaddeghi P. Aging: a cell source limiting factor in tissue engineering. *World Journal of Stem Cells* 2019;**11**:787–802.
14. Bachmann M, Moroy T. The serine/threonine kinase Pim-1. *The International Journal of Biochemistry & Cell Biology* 2005;**37**:726–730.
15. Scimè A, Desrosiers J, Trensz F, Palidwor GA, Caron AZ, Andrade-Navarro MA, et al. Transcriptional profiling of skeletal muscle reveals factors that are necessary to maintain satellite cell integrity during ageing. *Mechanisms of Ageing and Development* 2010;**131**:9–20.
16. Nga ME, Swe NN, Chen KT, Shen L, Lilly MB, Chan SP, et al. PIM-1 kinase expression in adipocytic neoplasms: diagnostic and biological implications. *International Journal of Experimental Pathology* 2010;**91**:34–43.
17. Sadkowski T, Ciecierska A, Majewska A, Oprządek J, Dasiewicz K, Ollik M, et al. Transcriptional background of beef marbling—novel genes implicated in intramuscular fat deposition. *Meat Science* 2014;**97**:32–41.
18. Park YK, Hong VS, Lee TY, Lee J, Choi JS, Park DS, et al. The novel anti-adipogenic effect and mechanisms of action of SGI-1776, a Pim-specific inhibitor, in 3T3-L1 adipocytes. *International Journal of Molecular Medicine* 2016;**37**:157–164.
19. Li Z, Lin F, Zhuo C, Deng G, Chen Z, Yin S, et al. PIM1 kinase phosphorylates the human transcription factor FOXP3 at serine 422 to negatively regulate its activity under inflammation. *The Journal of Biological Chemistry* 2014;**289**:26872–26881.
20. Yip-Schneider MT, Horie M, Broxmeyer HE. Transcriptional induction of pim-1 protein kinase gene expression by interferon gamma and posttranscriptional effects on costimulation with steel factor. *Blood* 1995;**85**:3494–3502.
21. Zhang Y, Lei W, Yan W, Li X, Wang X, Zhao Z, et al. MicroRNA-206 is involved in survival of hypoxia preconditioned mesenchymal stem cells through targeting Pim-1 kinase. *Stem Cell Research & Therapy* 2016;**7**:61.
22. Brioche T, Pagano AF, Py G, Chopard A. Muscle wasting and aging: experimental models, fatty infiltrations, and prevention. *Molecular Aspects of Medicine* 2016;**50**:56–87.
23. De Carvalho FG, Justice JN, Freitas EC, Kershaw EE, Sparks LM. Adipose tissue quality in aging: how structural and functional aspects of adipose tissue impact skeletal muscle quality. *Nutrients* 2019;**11**:2553.
24. Seo K, Suzuki T, Kobayashi K, Nishimura T. Adipocytes suppress differentiation of

muscle cells in a co-culture system. *Animal Science Journal* 2019;**90**:423–434.
25. Sun YN, Huang JQ, Chen ZZ, Du M, Ren FZ, Luo J, et al. Amyotrophy induced by a high-fat diet is closely related to inflammation and protein degradation determined by quantitative phosphoproteomic analysis in skeletal muscle of C57BL/6 J mice. *The Journal of Nutrition* 2020;**150**:294–302.
26. Brzeszczynska J, Meyer A, McGregor R, Schilb A, Degen S, Tadini V, et al. Alterations in the in vitro and in vivo regulation of muscle regeneration in healthy ageing and the influence of sarcopenia. *Journal of Cachexia, Sarcopenia and Muscle* 2018;**9**:93–105.
27. Sousa-Victor P, Muñoz-Cánoves P. Regenerative decline of stem cells in sarcopenia. *Molecular Aspects of Medicine* 2016;**50**: 109–117.
28. Arrighi N, Moratal C, Clément N, Giorgetti-Peraldi S, Peraldi P, Loubat A, et al. Characterization of adipocytes derived from fibro/adipogenic progenitors resident in human skeletal muscle. *Cell Death & Disease* 2015;**6**:e1733.
29. Buras ED, Converso-Baran K, Davis CS, Akama T, Hikage F, Michele DE, et al. Fibro-adipogenic remodeling of the diaphragm in obesity-associated respiratory dysfunction. *Diabetes* 2019;**68**:45–56.
30. Mogi M, Kohara K, Nakaoka H, Kan-No H, Tsukuda K, Wang XL, et al. Diabetic mice exhibited a peculiar alteration in body composition with exaggerated ectopic fat deposition after muscle injury due to anomalous cell differentiation. *Journal of Cachexia, Sarcopenia and Muscle* 2016;**7**:213–224.
31. Liu ZZ, Hong CG, Hu WB, Chen ML, Duan R, Li HM, et al. Autophagy receptor OPTN (optineurin) regulates mesenchymal stem cell fate and bone-fat balance during aging by clearing FABP3. *Autophagy* 2020;1–17. https://doi.org/10.1080/15548627.2020.1839286
32. Shen J, Zhu X, Liu H. MiR-483 induces senescence of human adipose-derived mesenchymal stem cells through IGF1 inhibition. *Aging (Albany NY)* 2020;**12**:15756–15770.
33. Gopal SS, Eligar SM, Vallikannan B, Ponesakki G. Inhibitory efficacy of lutein on adipogenesis is associated with blockage of early phase regulators of adipocyte differentiation. *Biochimica et Biophysica Acta - Molecular and Cell Biology of Lipids* 2021;**1866**:158812.
34. Liu Y, Shang Y, Yan Z, Li H, Wang Z, Liu Z, et al. Pim1 kinase positively regulates myoblast behaviors and skeletal muscle regeneration. *Cell Death & Disease* 2019;**10**:773.
35. von Haehling S, Morley JE, Coats AJS, Anker SD. Ethical guidelines for publishing in the Journal of Cachexia, Sarcopenia and Muscle: update 2019. *Journal of Cachexia, Sarcopenia and Muscle* 2019;**10**: 1143–1145.